Inorg. Chem. **2007**, *46*, 1675–1683

Diazene Dehydrogenation Follows H_2 Addition to Coordinated Dinitrogen in an *ansa*-Zirconocene Complex

Tamara E. Hanna, Ivan Keresztes, Emil Lobkovsky, and Paul J. Chirik*

Department of Chemistry and Chemical Biology, Baker Laboratory, Cornell University, Ithaca, New York 14853

Received October 26, 2006

An activated side-on-bound *ansa*-zirconocene dinitrogen complex, $[Me_2Si(\eta^5\text{-}C_5Me_4)(\eta^5\text{-}C_5H_3\text{-}3\text{-}^tBu)Zr]_2(\mu_2,\eta^2,\eta^2\text{-}N_2)$, has been prepared by sodium amalgam reduction of the corresponding dichloride precursor under an atmosphere of N_2. Both solution spectroscopic and X-ray diffraction data establish diastereoselective formation of the syn homochiral dizirconium dimer. Addition of 1 atm of H_2 resulted in rapid hydrogenation of the N_2 ligand to yield one diastereomer of the hydrido zirconocene diazenido complex. Kinetic measurements have yielded the barrier for H_2 addition and in combination with isotopic labeling studies are consistent with a 1,2-addition pathway. In the absence of H_2, the hydrido zirconocene diazenido product undergoes swift diazene dehydrogenation to yield an unusual hydrido zirconocene dinitrogen complex. The N═N bond length of 1.253(5) Å determined by X-ray crystallography indicates that the side-on-bound N_2 ligand is best described as a two-electron reduced $[N_2]^{2-}$ fragment. Comparing the barrier for deuterium exchange with $[Me_2Si(\eta^5\text{-}C_5Me_4)(\eta^5\text{-}C_5H_3\text{-}3\text{-}^tBu)ZrH]_2(\mu_2,\eta^2,\eta^2\text{-}N_2H_2)$ to diazene dehydrogenation is consistent with rapid 1,2-elimination of dihydrogen followed by rate-determining hydride migration to the zirconium. This mechanistic proposal is also corroborated by H_2 inhibition and the observation of a normal, primary kinetic isotope effect for dehydrogenation.

Introduction

Society's dependence on industrial ammonia production[1] coupled with the high energy costs associated with the Haber−Bosch process[2] inspire study into the mechanisms[3] by which N−H bonds are formed from their constituent elements. The observation of N_2 hydrogenation promoted by well-defined, soluble transition metal dinitrogen complexes[4−6] offers an unprecedented opportunity to explore new pathways for N−H bond formation. Ideally, the combined insight into N_2 hydrogenation coupled with N≡N bond cleavage may provide the foundation for new energy-efficient reactions that utilize atmospheric nitrogen as a chemical feedstock.[7]

Both metallocene[8] and non-metallocene[4] zirconium dinitrogen complexes have been reported that hydrogenate side-on-coordinated N_2 at 1 atm of H_2 pressure at ambient temperature. Both mechanistic[8] and computational studies[9] from our laboratory and others[10] on substituted bis(cyclopentadienyl) complexes support a 1,2-addition pathway, whereby H_2, terminal alkynes,[11] and saturated C−H bonds[8] undergo cycloaddition to a zirconium−nitrogen bond with significant imido character (eq 1). In the case of $[(\eta^5\text{-}C_5Me_4H)_2Zr]_2(\mu_2,\eta^2,\eta^2\text{-}N_2)$, continued hydrogenation at 85 °C produced small quantities of free ammonia.[6]

While a fairly mature understanding of the pathway of N_2 hydrogenation in zirconocene and hafnocene dinitrogen

* To whom correspondence should be addressed. E-mail: pc92@cornell.edu.

(1) Smil, V. *Enriching the Earth: Fritz Haber, Carl Bosch, and the Transformation of World Food Production*; MIT Press: Cambridge, MA, 2001.
(2) (a) Tamaru, K. In *Catalytic Ammonia Synthesis*; Jennings, J. R., Ed.; Plenum: New York, 1991. (b) Schlögl, R. *Angew. Chem., Int. Ed.* **2003**, *42*, 2004.
(3) Ertl, G. *Chem. Rec.* **2001**, 33.
(4) Fryzuk, M. D.; Love, J. B.; Rettig, S. J. *Science* **1997**, *275*, 1445.
(5) (a) Korobkov, I.; Gambarotta, S.; Yap, G. P. A. *Angew. Chem., Int. Ed.* **2003**, *42*, 4958. (b) Gilbertson, J. D.; Szymczak, N. D.; Tyler, D. R. *J. Am. Chem. Soc.* **2005**, *127*, 10184.
(6) Pool, J. A.; Lobkovsky; Chirik, P. J. *Nature* **2004**, *427*, 527.
(7) Mori, M. *J. Organomet. Chem.* **2004**, *689*, 4210.
(8) Bernskoetter, W. H.; Lobkovsky, E.; Chirik, P. J. *J. Am. Chem. Soc.* **2005**, *127*, 14051.
(9) Pool, J. A.; Bernskoetter, W. H.; Chirik, P. J. *J. Am. Chem. Soc.* **2004**, *126*, 14326.
(10) (a) Bobadova-Parvanova, P.; Wang, Q.; Morokuma, K.; Musaev, D. G. *Angew. Chem., Int. Ed.* **2005**, *44*, 7101. (b) Miyachi, H.; Shigeta, Y.; Hirao, K. *J. Phys. Chem. A* **2005**, *109*, 8800.
(11) Bernskoetter, W. H.; Pool, J. A.; Lobkovsky, E.; Chirik, P. J. *J. Am. Chem. Soc.* **2005**, *127*, 7901.

10.1021/ic0620539 CCC: $37.00
Published on Web 02/01/2007

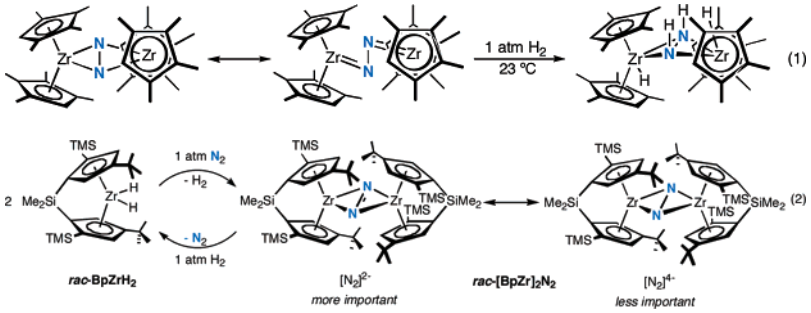

complexes has emerged,[12−14] many open questions remain. Efforts in our laboratory continue to explore structure−reactivity relationships for N−H bond formation in an attempt to determine what ligand environments are effective for imparting imido character into metal−nitrogen bonds. The objective of these studies is to not only find improved methods for ammonia synthesis but also to open new synthetic pathways for the elaboration of the N−N bond.[15]

Ansa-zirconocene complexes, whereby the two substituted cyclopentadienyl rings are tethered by at least one single- or multiatom bridge, are attractive for N_2 fixation, as these molecules often display unique or enhanced reactivity as compared to their unbridged counterparts.[16,17] The configurational stability of the ancillary ligand framework allows for the straightforward design and synthesis of side-on-bound dinitrogen complexes with canted dimeric cores to impart additional zirconium−N_2 backbonding.[9] For chiral metallocenes, the restricted ring rotation also provides an additional stereochemical probe to possibly answer open mechanistic questions surrounding dinitrogen hydrogenation and related functionalization reactions.

To our knowledge, only one *ansa*-zirconocene dinitrogen complex, [*rac*-(Bp)Zr]$_2$(μ_2,η^2,η^2-N_2) (Bp = $Me_2Si(\eta^5$-C_5H_2-2-$SiMe_3$-4-$^tBu_3)_2$), has been reported.[18] Unlike most zirconium dinitrogen compounds, [*rac*-(Bp)Zr]$_2$(μ_2,η^2,η^2-N_2) was prepared by reductive elimination of H_2 from the corresponding zirconocene dihydride. This synthetic method is a mild alternative to traditional alkali metal reduction procedures (eq 2).[19]

[*rac*-(Bp)Zr]$_2$(μ_2,η^2,η^2-N_2) is also unusual in that the side-on coordinated dinitrogen ligand is weakly activated as compared to other zirconocene N_2 complexes with η^2,η^2-hapticity.[20] In the solid state, the observed N−N bond distance of 1.2450(38) Å suggests a significant contribution from an $[N_2]^{2-}$ "diazenido" resonance form rather than the more reduced $[N_2]^{4-}$ "hydrazido" alternative. Antiferromagnetic coupling of the two formally Zr(III), d^1 centers via superexchange mediated by the Zr_2N_2 core accounts for the experimentally observed diamagnetism.[18]

The weak activation of the dinitrogen ligand in [*rac*-(Bp)Zr]$_2$(μ_2,η^2,η^2-N_2) is manifest in the reactivity of the compound. Addition of dihydrogen resulted in loss of the dinitrogen ligand, regenerating the starting zirconocene dihydride, *rac*-(Bp)ZrH_2 (eq 2).[18] These results serve to highlight the breaches in our current understanding of structure−reactivity relationships in the hydrogenation of side-on-bound zirconocene dinitrogen complexes and demonstrate that side-on coordination of the N_2 ligand is not the only prerequisite for hydrogenation and related cycloaddition chemistry.

In this contribution, we report the synthesis of an activated *ansa*-zirconocene dinitrogen complex and seek to answer open questions surrounding N_2 hydrogenation with soluble metal complexes. A sufficiently reducing environment has been achieved where the two zirconium centers in the dimer impart imido character into the zirconium−nitrogen bonds. Addition of H_2 resulted in rapid hydrogenation of the coordinated dinitrogen ligand. Removal of the dihydrogen atmosphere resulted in dehydrogenation of the newly formed diazene ligand to yield an unusual hydrido zirconocene dinitrogen complex. Kinetic and isotopic labeling studies have been used to explore the mechanism of this transformation.

Results and Discussion

Synthesis and Characterization of an Activated *Ansa*-Zirconocene Dinitrogen Complex. To prepare an *ansa*-zirconocene for dinitrogen functionalization by 1,2-addition of nonpolar reagents such as dihydrogen and C−H bonds, the substituents on the bis(cyclopentadienyl) framework must be carefully selected. The zirconium must be sufficiently exposed as to favor η^2,η^2-(side-on) hapticity of the dinitrogen ligand, as steric crowding is known to favor structures such as [(η^5-C_5Me_5)(η^5-C_5Me_4R)Zr(η^1-N_2)]$_2$(μ_2,η^1,η^1-N_2) (R = Me,[21] H[9]) that contain weakly activated η^1,η^1-(end-on) N_2 ligands. The cyclopentadienyl substituents must also be

(12) Bernskoetter, W. H.; Olmos, A. V.; Lobkovsky, E.; Chirik, P. J. *Organometallics* **2006**, *25*, 1021.
(13) Pool, J. A.; Chirik, P. J. *Can. J. Chem.* **2005**, *83*, 286.
(14) Chirik, P. J. *Dalton Trans.* **2007**, *1*, 16.
(15) Bernskoetter, W. H.; Olmos, A. V.; Pool, J. A.; Lobkovsky, E.; Chirik, P. J. *J. Am. Chem. Soc.* **2006**, *128*, 10696.
(16) Zachmanoglou, C. E.; Docrat, A.; Bridgewater, B. M.; Parkin, G. E.; Brandow, C. G.; Bercaw, J. E.; Jardine, C. N.; Lyall, M.; Green, J. C.; Kiester, J. B. *J. Am. Chem. Soc.* **2002**, *124*, 9525.
(17) (a) Lee, H.; Desrosiers, P. J.; Guzei, I.; Rheingold, A. L.; Parkin, G. *J. Am. Chem. Soc.* **1998**, *120*, 3255. (b) Lee, H.; Bridgewater, B. M.; Parkin, G. *J. Chem. Soc., Dalton Trans.* **2000**, 4490.
(18) Chirik, P. J.; Henling, L. M.; Bercaw, J. E. *Organometallics* **2001**, *20*, 534.
(19) For synthesis of early transition metal dinitrogen complexes by reductive elimination see: (a) Fryzuk, M. D.; Johnson, S. A.; Patrick, B. O.; Albinati, A.; Mason, S. A.; Koetzle, T. F. *J. Am. Chem. Soc.* **2001**, *123*, 3960. (b) Pool, J. A.; Lobkovsky, E.; Chirik, P. J. *Organometallics* **2003**, *22*, 2797. (c) Pool, J. A.; Lobkovsky, E.; Chirik, P. J. *J. Am. Chem. Soc.* **2003**, *125*, 2241. (d) de Wolf, J. M.; Blaauw, R.; Meetsma, A.; Teuben, J. H.; Gyepes, R.; Varga, V.; Mach, K.; Veldman, N.; Spek, A. L. *Organometallics* **1996**, *15*, 4977.
(20) MacLachlen, E. A.; Fryzuk, M. D. *Organometallics* **2006**, *25*, 1530.
(21) Manriquez, J. M.; Bercaw, J. E. *J. Am. Chem. Soc.* **1974**, *96*, 6229.

Table 1. Infrared Carbonyl Stretching Frequencies for Zirconocene Dicarbonyl Compounds

compound	$\nu(CO)_{sym}$ (cm^{-1})	$\nu(CO)_{asym}$ (cm^{-1})	$\nu(CO)_{avg}$ (cm^{-1})
1-(CO)$_2$	1960	1873	1916.5
rac-(Bp)Zr(CO)$_2$[16]	1967	1888	1927
2-(CO)$_2$[a]	1951	1858	1904.5
3-(CO)$_2$[b]	1952	1860	1906

[a] (η^5-C_5Me_4H)$_2$Zr(CO)$_2$, see ref 16. [b] (η^5-C_5Me_5)(η^5-C_5H_2-1,2-Me_2-4-Ph)Zr(CO)$_2$, see ref 8.

sufficiently large to "twist" the planes of the zirconocene wedges with respect to each other to achieve an appropriate dihedral angle for Zr_2N_2 backbonding.[9] The observation of N_2 dissociation upon addition of H_2 to [*rac*-(Bp)Zr]$_2$(μ_2,η^2,η^2-N_2) (wedge dihedral angle = 46.4°) suggests that other requirements remain to be uncovered. One possibility is that the cyclopentadienyl substituents need to be sufficiently electron donating to favor contribution from the four-electron reduced $[N_2]^{4-}$ hydrazido form.

With these specific design criteria and a new hypothesis in mind, an alkylated *ansa*-zirconocene dichloride complex, $Me_2Si(\eta^5\text{-}C_5Me_4)(\eta^5\text{-}C_5H_3\text{-}3\text{-}^tBu)ZrCl_2$ (**1-Cl$_2$**), was selected and prepared according to procedures described in the literature.[22] To evaluate the electronic environment imparted by this specific bis(cyclopentadienyl) ligand architecture, the zirconocene dicarbonyl complex[16] was prepared. Magnesium reduction of **1-Cl$_2$** under 4 atm of carbon monoxide in THF yielded a red solid identified as $Me_2Si(\eta^5\text{-}C_5Me_4)(\eta^5\text{-}C_5H_3\text{-}3\text{-}^tBu)Zr(CO)_2$ (**1-(CO)$_2$**) (eq 3).

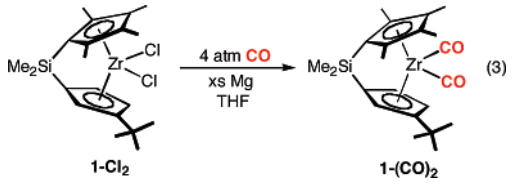

The infrared spectrum of **1-(CO)$_2$** was recorded in pentane solution, and the carbonyl stretching frequencies are reported in Table 1. As anticipated,[23] the more alkylated *ansa*-zirconocene dicarbonyl, **1-(CO)$_2$**, exhibits lower carbonyl stretching frequencies than silylated *rac*-(Bp)Zr(CO)$_2$,[16] signaling a more electron rich and hence more reducing zirconium center in the former case. Comparing the carbonyl stretching frequencies of the *ansa*-zirconocene dicarbonyls to the corresponding unconstrained bis(cyclopentadienyl) compounds reveals more electrophilic metal centers in the *ansa* derivatives.[16] The combination of an electron-withdrawing [$SiMe_2$]-bridge coupled with the reduction of the number of alkyl substituents is likely the origin of this effect.

Encouraged by the results from the infrared spectroscopic study that demonstrated that **1-(CO)$_2$** contained a more reducing zirconium center than *rac*-(Bp)Zr(CO)$_2$, the synthesis of the dinitrogen complex derived from reduction of **1-Cl$_2$** was targeted. Stirring **1-Cl$_2$** with an excess of 0.5% sodium amalgam in toluene under an atmosphere of dinitrogen followed by recrystallization from diethyl ether furnished green crystals identified as one diastereomer of [$Me_2Si(\eta^5\text{-}C_5Me_4)(\eta^5\text{-}C_5H_3\text{-}3\text{-}^tBu)Zr]_2(\mu_2,\eta^2,\eta^2\text{-}N_2$) (**1-N$_2$**) in 72% yield (eq 4). Because each zirconocene is chiral and

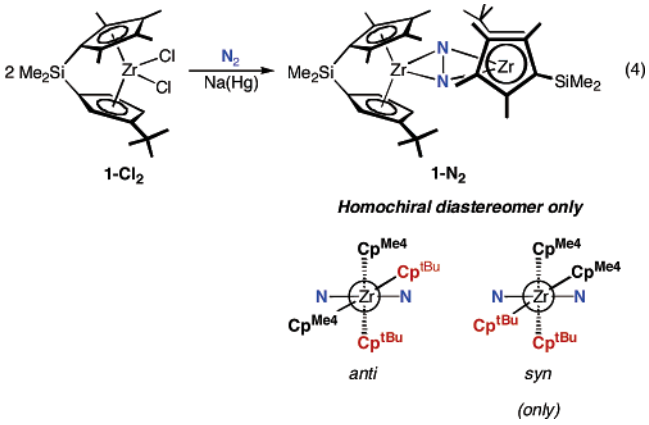

the dichloride precursor was used in racemic form, isolation of a dimeric product such as **1-N$_2$** offers the possibility for both homochiral and heterochiral diastereomers. A combination of multinuclear (^{1}H, ^{13}C, and ^{15}N) NMR experiments[24] and an X-ray diffraction study established exclusive formation of the syn-homochiral diastereomer, comprised of the (*SS*) and (*RR*) enantiomers.[25] The syn designator refers to the relative disposition of the cyclopentadienyl rings across the dimer and indicates the isomer where like rings are adjacent (eq 4). Note that if the two metallocene wedges were orthogonal, there would be no distinction between "anti" and "syn"; the deviation from idealized perpendicularity differentiates the two isomeric possibilities.[26]

The solid-state structure of **1-N$_2$** (Figure 1) established a side-on bound dinitrogen complex and confirmed the stereochemistry as the syn homochiral diastereomer. The *SS* enantiomer[27] is shown, and a representation of the *RR* complex is presented in the Supporting Information. The preference for formation of the syn homochiral dinitrogen complex is evident from the crystallographic data, as this conformation minimizes steric interactions between the *tert*-butyl substituents across the Zr_2N_2 core. In agreement with the carbonyl stretching frequencies, the N−N bond distance in **1-N$_2$** is elongated to 1.406(4) Å, consistent with a strongly activated, $[N_2]^{4-}$-type ligand. The two halves of the dimer

(22) Antiñolo, A.; López-Solera, I.; Otero, A.; Prashar, S.; Rodríguez, A. M.; Villaseñor, E. *Organometallics* **2002**, *21*, 2460.
(23) Bradley, C. A.; Flores-Torres, S.; Lobkovsky, E.; Abruña, H. D.; Chirik, P. J. *Organometallics* **2004**, *23*, 5332.
(24) See Supporting Information for complete details of all spectral assignments.
(25) For simplicity, only one enantiomer (*SS*) is shown in all drawings.
(26) In the static limit, each homochiral dimer has the possibility of distinct conformers. Sighting down the Zr−Zr vector, clockwise rotation away from a dihedral angle of 0° gives the positive synclinal conformation, while counterclockwise rotation yields the negative synclinal conformation. Because only one set of peaks for the homochiral diastereomer is observed by NMR spectroscopy, a fluxional process occurs in solution to rapidly interconvert the conformers. For a discussion of synclinal and anticlinal conformers see: Carroll, F. A. *Perspectives on Structure and Mechanism in Organic Chemistry*; Brooks-Cole: Pacific Grove, CA, 1998; pp 121−122.
(27) For assignment of the (*R*) and (*S*) Cahn−Ingold−Prelog designators in *ansa*-metallocenes see: Halterman, R. L. In *The Metallocenes*; Togni, A., Halterman, R. L., Eds.; Wiley-VCH: New York, 1998; Vol. 1, pp 461−468.

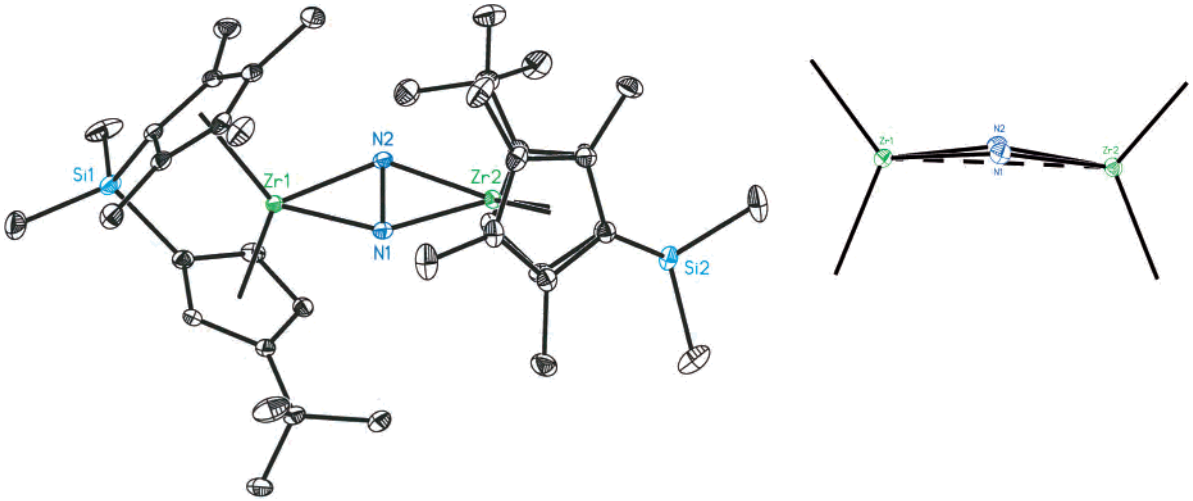

Figure 1. Partially labeled view of the molecular structure of **(*SS*)-1-N_2** at 30% probability ellipsoids (left). Core of the molecule (right). Hydrogen atoms omitted for clarity.

Table 2. Structural Parameters for Side-On Bound Bis(cyclopentadienyl)Zirconium Dinitrogen Compounds

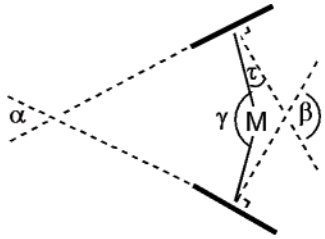

$\alpha = 180 - \beta$; $\alpha = 2\tau - \gamma$; $\tau = 0.5(\gamma - \beta)$

	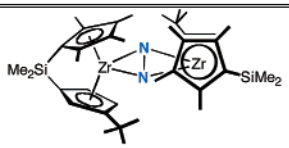 **1-N_2**	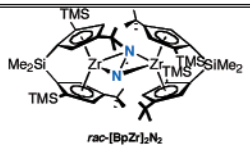 ***rac*-[BpZr]$_2$N$_2$**	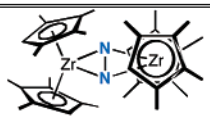 **2-N_2**	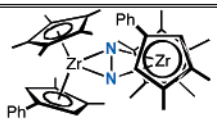 **3-N_2**
α[a]	60.2	61.7	49.1	48.7
β	119.8	118.3	130.9	131.3
γ	125.5	125.1	128.4	131.0
τ	2.9	3.4	-1.3	-2.0
ϕ[b]	54.1	46.4	65.3	72.9
Zr_2N_2 dev[c]	12.8	0.0	0.0	3.1

[a] All values reported in degrees. [b] Dihedral angle formed between the planes of the zirconium and the cyclopentadienyl centroids. [c] Deviation from the idealized plane defined by the Zr_2N_2 core.

are significantly twisted with respect to one another with an observed dihedral angle of 54.1°, as defined by the planes formed by the zirconium and the two cyclopentadienyl centroids. Notably, the Zr_2N_2 core of the molecule is slightly puckered by 12.8°, contrasting related side-on bound zirconocene complexes with planar metal−dinitrogen fragments.[8,18]

To determine the influence of the *ansa* bridge on the ground-state structure of Group 4 metallocene dinitrogen complexes, the metrical and electronic parameters of **1-N_2** were compared to other known bis(cyclopentadienyl)zirconium derivatives. Presented in Table 2 is a comparison of structural parameters for **1-N_2**, [*rac*-(Bp)Zr]$_2$(μ_2,η^2,η^2-N_2), [(η^5-C_5Me_4H)$_2$Zr]$_2$(μ_2,η^2,η^2-N_2) (**2-N_2**), and [(η^5-C_5Me_5)(η^5-C_5H_2-1,2-Me_2-4-Ph)Zr]$_2$(μ_2,η^2,η^2-N_2) (**3-N_2**).

As noted previously in zirconocene dichlorides,[16] introduction of an [$SiMe_2$] *ansa* bridge results in a modest contraction of the Cp_{cent}−M−Cp_{cent} (γ) angle from its more relaxed value in the corresponding unconstrained compounds. For the series of dinitrogen complexes presented in Table 2, the [$SiMe_2$] bridge does contract γ; however, caution must be exercised in attributing these differences to an "*ansa* effect", as the cyclopentadienyl substituents are markedly different. Another notable structural difference in the series of zirconocene dinitrogen compounds presented in Table 2 is the expansion of the inter-ring angle, α, between the *ansa* and

Table 3. LMCT Bands and Extinction Coefficients for Side-On Bound Zirconocene Dinitrogen Complexes Recorded in Heptane Solution

compound[a]	λ_{max} (nm)	ϵ (M^{-1} cm^{-1})
1-N_2	1015	9900
2-N_2[b]	1006	11 400
3-N_2[c]	1046	9200
4-N_2[d]	1014	8900

[a] Values for **2-N_2**, **3-N_2**, and **4-N_2** taken from ref 8. [b] [(η^5-C_5Me_4H)$_2$Zr]$_2$(μ_2,η^2,η^2-N_2). [c] [(η^5-C_5Me_5)(η^5-C_5H_2-1,2-Me_2-4-Ph)Zr]$_2$(μ_2,η^2,η^2-N_2). [d] [(η^5-C_5Me_5)(η^5-C_5H_2-1,2,4-Me_3)Zr]$_2$(μ_2,η^2, η^2-N_2).

Table 4. Relative Rates of Hydrogenation and Kinetic Isotope Effects for Side-On Bound Zirconocene Dinitrogen Complexes

compound	k_{obs} (s^{-1})[a]	k_{rel}	k_H/k_D
1-N_2	$3.7(3) \times 10^{-3}$	3.9	2.4(3)
2-N_2	$3.9(4) \times 10^{-3}$	4.1	2.4(2)
3-N_2	$9.5(1) \times 10^{-4}$	1.0	1.8(3)
4-N_2	$1.2(1) \times 10^{-3}$	1.3	2.2(2)

[a] Determined at 0.647 atm of H_2 at 23 °C in heptane solution.

unconstrained compounds. Because α and β are supplementary angles (i.e., α + β = 180), β contracts accordingly. Taken together, these data suggest that the *ansa*-zirconocene dinitrogen compounds are slightly more open than their unconstrained counterparts.

Kinetics and Stereochemistry of Hydrogenation of *ansa*-Zirconocene Dinitrogen Complexes. The hydrogenation chemistry of **1-N_2** was explored to demonstrate the impact of the more reduced dinitrogen ligand on the reactivity of the complex. Exposure of **1-N_2** to 1 atm of dihydrogen at 23 °C resulted in isolation of a yellow solid identified as a single diastereomer of the hydrido zirconocene diazenido compound, [Me_2Si(η^5-C_5Me_4)(η^5-C_5H_3-3-^{t}Bu)ZrH]$_2$(μ_2,η^2,η^2-N_2H_2) (**1-N_2H_4**) (eq 5). Recall that hydrogenation of the more

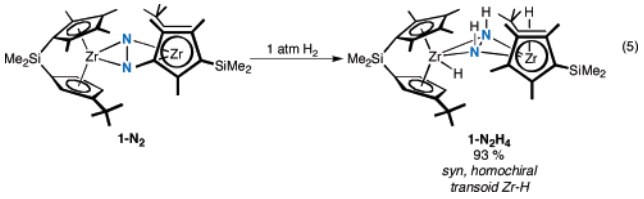

(5)

weakly activated side-on-bound dinitrogen complex, [*rac*-(Bp)Zr]$_2$(μ_2,η^2,η^2-N_2),[18] induced N_2 loss and formation of the corresponding zirconocene dihydride.

The pyramidalized nitrogens of the diazenido core and the position of the hydrides with respect to both the cyclopentadienyl ligands and to each other offers the possibility for a myriad of isomers. The ^{1}H NMR spectrum of **1-N_2H_4** exhibits the number of resonances expected for only one C_2-symmetric compound. On the basis of NOESY NMR spectroscopic data, the observed isomer was assigned as the syn homochiral dimer with transoid hydride ligands (eq 5). Complete details of the spectral assignment are described in the Supporting Information. Similar to **1-$^{15}N_2$** where one ^{15}N NMR resonance centered at 603.5 ppm was detected, observation of one cross-peak in the ^{1}H−^{15}N HSQC NMR spectrum centered at 71.2 ppm of **1-$^{15}N_2H_4$** is also consistent with formation of one C_2-symmetric product where the two nitrogen atoms of the diazenido ligand are related by the principal axis. The relative upfield chemical shift of the ^{15}N resonance in addition to the ^{1}H NMR shift at 1.34 ppm for the N−*H* resonance is consistent with η^2,η^2 hapticity of the N_2H_2 core.[11] Monitoring the shift of the N−H resonance as a function of raising the temperature to 95 °C produced no change and suggests that end-on diazenido isomers are not sufficiently populated in solution.[11]

The stereochemistry of the observed hydrogenation product is consistent with consecutive 1,2-addition reactions from the sole isomer of **1-N_2**, in agreement with previous mechanistic studies. If competing isomerization processes are not operative, the stereochemistry of **1-N_2H_4** suggests that the H_2 molecules approach the zirconocene from the side of the wedge that bears the *tert*-butyl cyclopentadienyl substituent and highlight the utility of using configurationally stable *ansa*-metallocenes to monitor the stereochemistry of H_2 addition. It should also be noted that the steric difficulties associated with approach to the more hindered side of the zirconocene may be attenuated by conformational fluxionality.

Having elucidated the stereochemistry of H_2 addition, the rate of N_2 hydrogenation was explored with the goal of determining if an "*ansa*-effect" was operative. As described previously,[8] monitoring the disappearance of characteristic ligand-to-metal charge transfer (LMCT) bands of a side-on-bound zirconocene dinitrogen complex as a function of time by electronic spectroscopy has proven to be a reliable method for determining pseudo-first-order rate constants for N_2 hydrogenation. The *ansa* complex **1-N_2** exhibits a strong LMCT band centered at 1015 nm with an extinction coefficient of 9900 M^{-1} cm^{-1}. Values in this range are similar to those reported for other side-on-bound zirconocene dinitrogen complexes (Table 3).

Using this technique, the pseudo-first-order rate constant (Table 4) for the hydrogenation of **1-N_2** at 23 °C with 0.647 atm of H_2, corresponding to an excess of greater than 5000 equiv total (17 equiv in solution),[28] was determined. The value of k_{obs} for the *ansa*-zirconocene dinitrogen compound is slightly larger than those previously reported for **3-N_2** and **4-N_2** but statistically indistinguishable from that for **2-N_2**.[8] Rationalizing the origin of such a small trend is tenuous but is most likely a consequence of the more open metallocene environment imparted by the *ansa*-bridge.

The rate law for the hydrogenation reaction[8] was established by measuring the pseudo-first-order rate constants for H_2 addition over a range of dihydrogen pressures. A minimum dihydrogen pressure of 0.400 atm (100.1 mL) was used as lower pressures of gas did not maintain pseudo-first-order kinetics. A linear correlation (R^2 = 0.997) between observed rate constant and dihydrogen pressure (Figure 2) was obtained and establishes a first-order dependence on H_2 concentration (pressure). These data in combination with the observed first-order dependence on **1-N_2** establish an overall second-order reaction, first order with respect to each reagent.

(28) *Solubility data series*, 1st ed.; Young, C. L., Ed; International Union of Pure and Applied Chemistry: Research Triangle Park, NC, 1981; Vol 5.

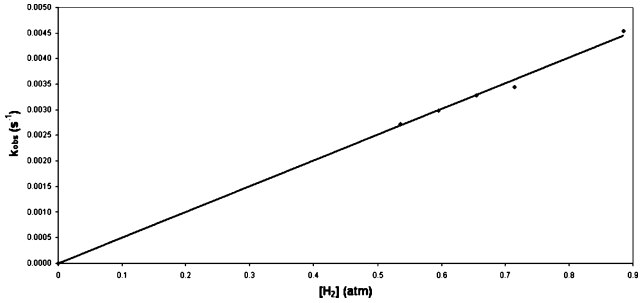

Figure 2. Plot of k_{obs} vs H_2 pressure for the hydrogenation of **1-N$_2$** at 23 °C.

The kinetic isotope effect for N_2 hydrogenation was also determined by measuring the rate constants for H_2 versus D_2 addition to **1-N$_2$** at an H_2 (or D_2) pressure of 0.647 atm (100.1 mL, Table 4). From these experiments, a normal, primary kinetic isotope effect of 2.4(3) was measured for **1-N$_2$**. Rate constants were collected over a 41 °C temperature range at 0.704 atm of H_2, and an Eyring plot[24] from the experimental data yielded activation parameters of $\Delta H^{\ddagger} = 6.2(6)$ kcal mol^{-1} and $\Delta S^{\ddagger} = -37(4)$ eu. These data, in combination with the observed first-order dependence on dihydrogen, are consistent with the first 1,2-addition of H_2 as rate determining and are analogous to the previously reported reaction coordinate based on both experimental[8] and computational results.[10b] Importantly, these data serve as an important reference point for the free energy diagram for the first H_2 addition step and provide a foundation for subsequent mechanistic studies on diazene dehydrogenation.

Dehydrogenation Chemistry of 1-N$_2$H$_4$. If handled appropriately, samples of **1-N$_2$H$_4$** can be isolated in the solid state. However, stirring a pentane or toluene solution of **1-N$_2$H$_4$** under a dinitrogen atmosphere or under vacuum at 23 °C resulted in loss of 1 equiv of dihydrogen, confirmed via Toepler pump. The resulting organometallic product was identified as the hydrido zirconocene dinitrogen complex, [Me$_2$Si(η^5-C$_5$Me$_4$)(η^5-C$_5$H$_3$-3-^{t}Bu)ZrH]$_2$(μ_2,η^2,η^2-N$_2$) (**1-H$_2$N$_2$**, eq 6). Preparative-scale syntheses of **1-H$_2$N$_2$** were routinely

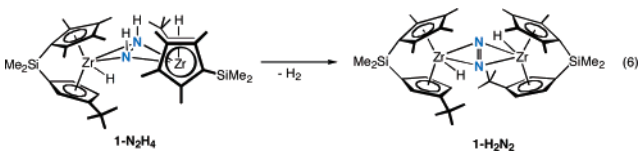

(6)

accomplished at slightly higher temperatures, typically 55 °C, and allowed isolation of the desired product as red-orange crystals in moderate yield.

The benzene-d_6 ^{1}H NMR spectrum of **1-H$_2$N$_2$** exhibits the number of cyclopentadienyl resonances for one diastereomer of a C_2-symmetric zirconocene dinitrogen complex. A singlet centered at 4.48 ppm was assigned as the transoid zirconium hydrides, and this resonance disappears upon preparation of **1-D$_2$N$_2$** from **1-N$_2$D$_4$**. The retention of zirconium dihydrides following H_2 loss was confirmed by benzene-d_6 solution IR spectroscopy, as a medium-intensity Zr−*H* band was located at 1543 cm^{-1}. This peak shifts appropriately to 1108 cm^{-1} upon preparation of **1-D$_2$N$_2$**.

^{15}N NMR spectroscopy has also proven diagnostic for detecting diastereoselective diazene dehydrogenation. Loss of H_2 from **1-^{15}N$_2$H$_4$**, prepared from hydrogenation of **1-^{15}N$_2$**, produced **1-H$_2$^{15}N$_2$**. The benzene-d_6 ^{15}N NMR spectrum of the compound exhibited a single resonance centered at 655.04 ppm, comparable to the typical downfield shifts observed for side-on-bound zirconium dinitrogen complexes.[14,20] The observation of a single ^{15}N NMR resonance supports a C_2-symmetric structure where the two nitrogen atoms are related by the rotational axis. Furthermore, the downfield shifting of the ^{15}N resonance also supports diazene dehydrogenation, as η^2,η^2-[N$_2$H$_2$]$^{2-}$ ligands bound to zirconocenes typically exhibit ^{15}N peaks in the vicinity of 90−110 ppm relative to liquid ammonia.[11]

The solid-state structure (Figure 3) confirmed the identity of the diastereomer of **1-H$_2$N$_2$** proposed from the solution spectroscopic data. The data were of sufficient quality such that the zirconium hydrides could be located and refined. As was observed in the solid-state structure of **1-N$_2$**, the cyclopentadienyl ligands in **1-H$_2$N$_2$** are in a syn orientation most likely to avoid steric interactions between the *tert*-butyl substituents across the dimer. Isolation of this diastereomer also indicates that no stereochemical scrambling of the ligand environments occurs during N_2 hydrogenation or diazene dehydrogenation. The N−N bond length has contracted to 1.253(5) Å, consistent with a two-electron reduced [N$_2$]$^{2-}$ ligand, similar to the corresponding distance in [*rac*-(Bp)-Zr]$_2$(μ_2,η^2,η^2-N$_2$). The transoid hydrides complete the coordination sphere of each zirconocene and are located on the same side of the metallocene wedges as the *tert*-butyl substituents. The wedge dihedral angle of 34.0° is also smaller than in **1-N$_2$** and serves to minimize steric interactions between the *tert*-butyl substituents across the dimer.

Full-molecule DFT calculations were performed on **1-H$_2$N$_2$** using the X-ray coordinates as the starting geometry with the goal of determining the frontier molecular orbitals of the complex. A partial molecular orbital diagram is presented in Figure 4. The computed HOMO of **1-H$_2$N$_2$** is a linear combination consisting principally of zirconocene b_2 orbitals with the in-plane N_2 π^* molecular orbitals. The computed LUMO, calculated to be ∼45 kcal mol^{-1} higher in energy than the HOMO, is essentially composed of the perpendicular N_2 π^* molecular orbitals that are nonbonding with respect to each metallocene unit. The planarity of the Zr_2N_2 core in combination with availability of only one electron from each metal center is the origin of the weak activation observed in the solid-state structure of **1-H$_2$N$_2$**.

The reversibility of diazene dehydrogenation was also explored. Treatment of **1-H$_2$N$_2$** with 4 atm of dihydrogen at 23 °C produced no detectable change by ^{1}H NMR spectroscopy. Warming the sample to 55 °C resulted in partial conversion to **1-N$_2$H$_4$**, but significant decomposition to unidentified zirconocene compounds was also observed. Performing the hydrogenation of **1-H$_2$N$_2$** at 130 °C resulted in dinitrogen loss and isolation of the zirconocene dihydride dimer, {[Me$_2$Si(η^5-C$_5$Me$_4$)(η^5-C$_5$H$_3$-3-^{t}Bu)ZrH$_2$]$_2$ (**1-H$_2$**) as a mixture of two isomers (eq 7). The major isomer, comprising 68% of the mixture, was identified by NOESY

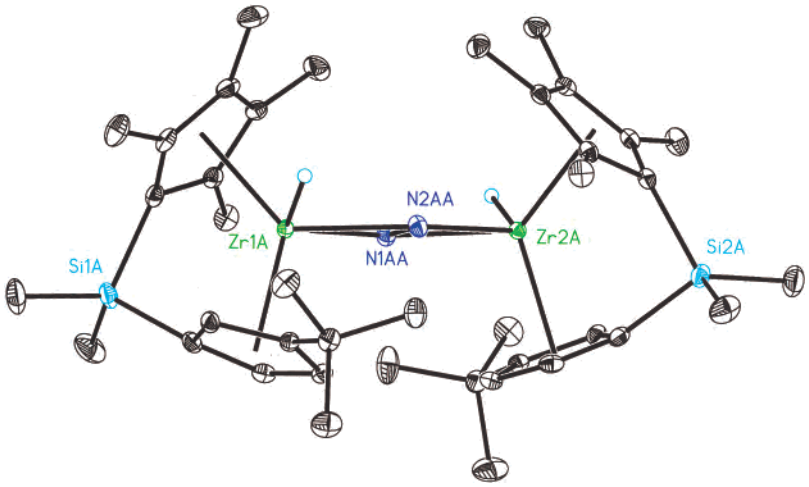

Figure 3. Molecular structure of **(*SS*)-1-H_2N_2** at 30% probability ellipsoids. Hydrogen atoms, except for the zirconium hydride positions, omitted for clarity. A view of the other enantiomer is presented in the Supporting Information.

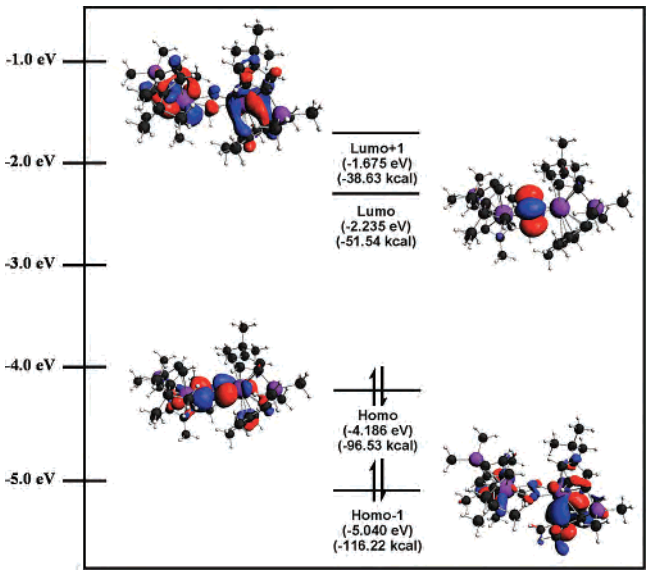

Figure 4. DFT-computed (ADF2004.01, TZ2P, ZORA) frontier molecular orbitals of **1-H_2N_2**.

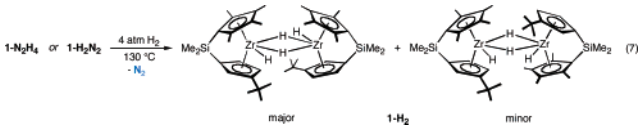

NMR spectroscopy as the syn homochiral diastereomer with transoid hydride ligands. The minor isomer, accounting for 32% of the isomeric mixture, is the anti homochiral dimer with cisoid zirconium hydrides. Similar products were obtained upon continued hydrogenation of **1-N_2H_4** at 130 °C. Notably, no ammonia was detected either by indophenolic titration or by ^{1}H NMR spectroscopy and is most likely a consequence of a more electron deficient zirconium center arising from coordination of the *ansa*-cyclopentadienyl ligand.

The mechanism of diazene dehydrogenation arising from **1-N_2H_4** was studied with a series of kinetic and isotopic labeling studies. The conversion of **1-N_2H_4** to **1-H_2N_2** under vacuum in benzene-d_6 at 55 °C follows clean first-order kinetics with a rate constant (k_H) of 1.6(1) $\times$ 10^{-4} s^{-1}. The corresponding experiment with the deuterated isotopologue, **1-N_2D_4**, yielded a first-order rate constant (k_D) of 4.4(1) $\times$ 10^{-5} s^{-1}, establishing a normal, primary kinetic isotope effect of 3.6(1) at this temperature. A KIE value of this direction and magnitude is consistent with N−H or Zr−H bond breaking in or prior to the rate-determining step of diazene dehydrogenation. Unlike the unconstrained complexes,[9] no deuterium exchange into the cyclopentadienyl substituents was observed under these conditions, demonstrating that the experimentally determined isotope effect is not compromised by competing cyclometalation reactions.

The influence of excess dihydrogen on the rate of conversion of **1-N_2H_4** to **1-H_2N_2** was also studied. Each experiment was conducted in a thick-walled glass vessel at constant volume with sufficient headspace such that a large excess of H_2 was present with respect to zirconium. For experimental convenience, the half-life of the conversion of **1-N_2H_4** to **1-H_2N_2** was used as a measure of the rate of the reaction. As reported in Table 5, the dehydrogenation of **1-N_2H_4** is inhibited by excess dihydrogen. At low dihydrogen pressures (0.46 atm), relatively swift diazene dehydrogenation is observed with a half-life of ~170 min. As the pressure is increased, the half-life of the dehydrogenation reaction also increases, consistent with an inverse dependence on H_2 pressure.

The temperature dependence of the rate constant for the conversion of **1-N_2H_4** to **1-H_2N_2** was determined over a 51 °C temperature range (23−74 °C) under vacuum. The Eyring plot from these data is presented in Figure 5. The linear fit to the data yielded an enthalpy of activation ($\Delta H^{\ddagger}$) of 26.8(3) kcal mol^{-1} and an entropy of activation ($\Delta S^{\ddagger}$) of 5.5(4) eu, consistent with a unimolecular process.

On the basis of the experimental data, a mechanism for diazene dehydrogenation (Figure 6) was proposed. Initial 1,2-elimination of dihydrogen initiates the reaction and may occur either from a side-on or end-on haptomer of **1-N_2H_4**. Variable-temperature ^{1}H NMR studies on **1-N_2H_4** demonstrate that η^1,η^1 isomers are not present at a detectable concentration in solution but could be populated along the reaction coordinate for dehydrogenation. Side-on, end-on

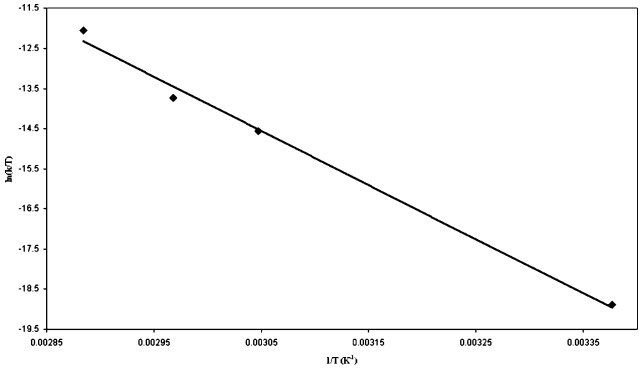

Figure 5. Eyring plot for the dehydrogenation of **1-N_2H_4**.

Table 5. Half-Lives for the Conversion of **1-N_2H_4** to **1-H_2N_2** as a Function of Dihydrogen Pressure

pressure H_2 (atm)	half life (min)
0.46	170
1.0	382
3.8	1510

isomerization of the $[N_2H_2]^{2-}$ ligand may be operative to achieve the required syn periplanar arrangement of the two hydrogen atoms required for 1,2-elimination. Following initial hydrogen loss, transfer of the N−*H* to the zirconium occurs by β-hydrogen elimination,[29] although if the intermediate remains in an η^2,η^2 ("closed") form, then the process could be viewed as an α-migration.

Additional experiments were conducted to determine the rate-determining step in the conversion **1-N_2H_4** to **1-H_2N_2**. The rate of 1,2-elimination was independently probed by measuring the rate constant for isotopic exchange upon addition of excess D_2 gas to **1-N_2H_4** (eq 8). To avoid potential

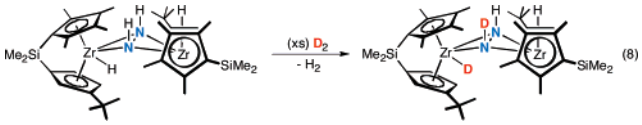

complications from secondary isotope effects, rate constants were determined by the method of initial rates, integrating the disappearance of the zirconium hydride resonance at early conversions. Using this approach, a pseudo-first-order rate constant of $3.1(5) \times 10^{-7}$ s^{-1} was measured at 20.5 °C. As with D_2 addition to **1-N_2H_4**, no deuterium incorporation into the cyclopentadienyl substituents was detected, demonstrating that competing cyclometalation processes are not operative at these temperatures.

Because competing cyclometalation pathways have not been detected, the relative rates of isotopic exchange as compared to that for diazene dehydrogenation establish the rate-determining step for the conversion of **1-N_2H_4** to **1-H_2N_2**. Special care must be taken to compare rates under the same standard state conditions. Four atmospheres of dihydrogen (dideuterium) at ambient temperature were chosen for experimental convenience. Under these conditions, dehydrogenation of **1-N_2H_4** to **1-H_2N_2** is exceedingly slow, reaching only 17% conversion after 903 h (37.6 days). By way of comparison, the corresponding deuterium exchange reaction with **1-N_2H_4** reaches this level of conversion in only 2.2 h, demonstrating that 1,2-elimination is much faster than overall diazene dehydrogenation. Therefore, these data, along with the observed kinetic isotope effect and inverse dependence on dihydrogen pressure, support a mechanism whereby rapid and reversible 1,2-elimination and addition precedes rate-determining N−H transfer by β-hydrogen elimination.

Concluding Remarks

Introduction of electron-donating alkyl substituents onto the cyclopentadienyl rings furnished a sufficiently reducing *ansa*-zirconocene that promotes the four-electron reduction of coordinated dinitrogen. This ground-state effect translates onto the hydrogenation chemistry of the compound, where addition of H_2 affords the hydrido zirconocene diazenido complex. Notably, the synthesis of the zirconocene dinitrogen complex and its hydrogenated product are diastereoselective. Only homochiral dimers where like cyclopentadienyl rings are adjacent were observed. In the absence of H_2, the diazenido core of the hydrogenated product undergoes loss of dihydrogen to yield a new hydrido zirconocene dinitrogen complex where the side-on-bound N_2 ligand is reduced by two electrons. Both kinetic and isotopic labeling experiments for diazene dehydrogenation are consistent with a rapid preequilibrium involving reversible dihydrogen loss and readdition followed by rate-determining β-hydrogen elimination.

Experimental Section[30]

Preparation of ([$Me_2Si(\eta^5$-$C_5Me_4)(\eta^5$-C_5H_3-^{t}Bu)]Zr)$_2(\mu_2,\eta^2,\eta^2$-$N_2)$ (1-N_2). A 100 mL round-bottomed flask was charged with 22.61 g of 0.5% sodium amalgam and ~15 mL of toluene. With vigorous

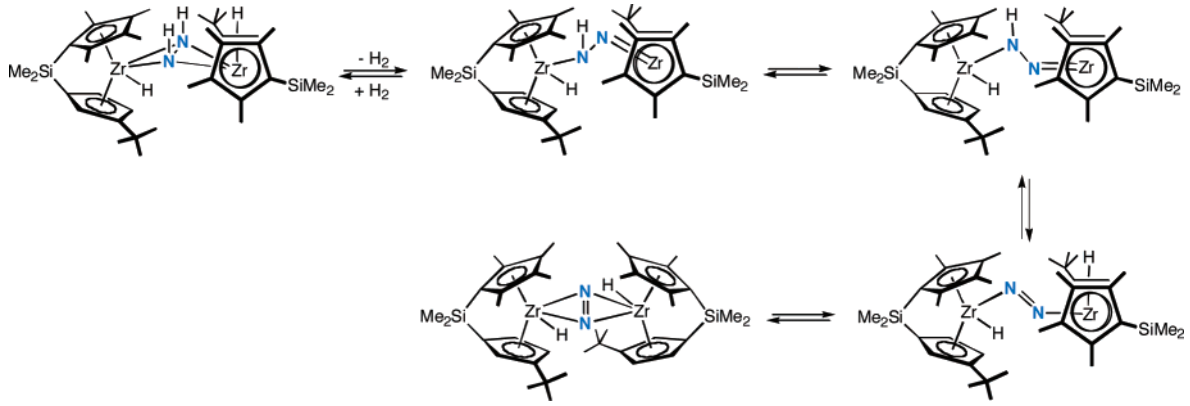

Figure 6. Proposed mechanism for the dehydrogenation of **1-N_2H_4**.

stirring, 0.450 g (0.977 mmol) of [$Me_2Si(\eta^5$-$C_5Me_4)(\eta^5$-C_5H_3-^{t}Bu)]-$ZrCl_2$ was added as a yellow toluene solution, and the resulting reaction mixture was stirred for 3 days at ambient temperature. The resulting green solution was filtered through a pad of Celite, and the solvent was removed in vacuo, leaving a green solid. Recrystallization from diethyl ether yielded 0.283 g (72%) of **1-N_2**. Anal. Calcd for $C_{40}H_{60}N_2Si_2Zr_2$: C, 59.49; H, 7.49; N, 3.47. Found: C, 59.04; H, 7.20; N, 3.06. ^{1}H NMR (benzene-d_6): δ 0.55 (s, 3H, SiMe_2), 0.67 (s, 3H, SiMe_2), 1.39 (s, 9H, $C_5H_3CMe_3$), 1.80 (s, 3H, C_5Me_4), 2.04 (s, 3H, C_5Me_4), 2.13 (s, 3H, C_5Me_4), 2.15 (s, 3H, C_5Me_4), 5.76 (s, 2H, $C_5H_3CMe_3$), 5.80 (s, 1H, $C_5H_3CMe_3$). ^{13}C NMR (benzene-d_6): δ −0.81, 0.59 (SiMe_2), 11.75, 12.22, 14.41, 14.53 (C_5Me_4), 31.57 (CMe_3), 32.88 (CMe$_3$), 106.89, 108.23, 109.10, 109.50, 109.88, 117.61, 118.07, 120.33, 130.10, 147.27 (Cp). ^{15}N NMR (benzene-d_6): δ 603.47 ($^{15}N_2$).

Preparation of ([$Me_2Si(\eta^5$-$C_5Me_4)(\eta^5$-C_5H_3-^{t}Bu)]ZrH)$_2(\mu_2,\eta^2,\eta^2$-N_2H_2) (1-N_2H_4). A thick-walled glass vessel was charged with 0.030 g (0.037 mmol) of **1-N_2** and ∼5 mL of a 50:50 mixture of pentane and toluene was added. On the high-vacuum line, the vessel was frozen in liquid nitrogen and evacuated. At −196 °C, 1 atm of hydrogen was added. The contents of the vessel were thawed and stirred overnight at room-temperature producing a color change from green to yellow. The solvent was removed in vacuo, leaving a yellow solid. The solid was transferred into the drybox and washed with pentane, and the solvent was removed in vacuo, yielding 0.028 g (93%) of a yellow solid identified as **1-N_2H_4**. Anal. Calcd for $C_{40}H_{64}N_2Si_2Zr_2$: C, 59.20; H, 7.95; N, 3.45. Found: C, 58.93; H, 7.68; N, 3.21. ^{1}H NMR (benzene-d_6): δ 0.53 (s, 3H, SiMe_2), 0.58 (s, 3H, SiMe_2), 1.34 (bs, 1H, N-*H*), 1.38 (s, 3H, C_5Me_4), 1.55 (s, 9H, $C_5H_3CMe_3$), 2.04 (s, 3H, C_5Me_4), 2.11 (s, 6H, C_5Me_4), 4.36 (s, 1H, Zr-*H*), 5.47 (s, 1H, $C_5H_3CMe_3$), 5.75 (s, 1H, $C_5H_3CMe_3$), 6.11 (s, 1H, $C_5H_3CMe_3$). ^{2}H NMR (benzene): δ 1.23 (N−*D*), 4.35 (Zr-*D*). ^{13}C NMR (benzene-d_6): δ −0.91, 0.75 (SiMe_2), 11.09, 13.58, 16.09 (C_5Me_4), 32.38 (CMe_3), 32.66 (CMe$_3$), 99.96, 101.65, 107.27, 109.10, 111.44, 119.56, 129.28, 149.30 (Cp). *One overlapping $CpMe_4$. Two Cp peaks not located.* IR (benzene-d_6): ν, 1549 (Zr−H), 1125 cm^{-1} (Zr−D). ^{15}N NMR (benzene-d_6): δ 71.2 (^{15}N−H).

(29) Schrock, R. R. *Acc. Chem. Res.* **2005**, *38*, 955.
(30) General considerations and additional experimental procedures are reported in the Supporting Information.

Preparation of [$Me_2(Si(\eta^5$-$C_5Me_4)(\eta^5$-C_5H_3-^{t}Bu)Zr]$_2H_2(\mu_2,\eta^2,\eta^2$-$N_2$) (1-$H_2N_2$). A thick-walled glass vessel was charged with 0.050 g (0.062 mmol) of **1-N_2** and ∼5 mL of a 50:50 mixture of pentane and toluene was added. On the high-vacuum line, the vessel was degassed and 1 atm of hydrogen was added at −196 °C. The reaction was stirred for 15 min, until a color change from green to yellow was observed. The contents of the vessel were frozen in liquid nitrogen, and the excess hydrogen gas was removed. The contents of the vessel were thawed and stirred overnight in a 45 °C oil bath, producing a color change from yellow to red-orange. The solvent was removed in vacuo, leaving a red solid. The solid was transferred into the drybox and dissolved in toluene, and then the solvent was removed. Recrystallization from a pentane/toluene mix resulted in 0.045 g (90%) of **1-H_2N_2**. Anal. Calcd for $C_{40}H_{62}N_2Si_2Zr_2$: C, 59.34; H, 7.72; N, 3.46. Found: C, 58.98; H, 7.31; N, 3.31. ^{1}H NMR (benzene-d_6): δ 0.52 (s, 3H, SiMe_2), 0.66 (s, 3H, SiMe_2), 1.26 (s, 3H, C_5Me_4), 1.68 (s, 9H, $C_5H_3CMe_3$), 1.94 (s, 3H, C_5Me_4), 2.09 (s, 3H, C_5Me_4), 2.75 (s, 3H, C_5Me_4), 4.48 (s, 1H, Zr-*H*), 4.67 (s, 1H, $C_5H_3CMe_3$), 5.42 (s, 1H, $C_5H_3CMe_3$), 5.63 (s, 1H, $C_5H_3CMe_3$). ^{13}C NMR (benzene-d_6): δ −0.64, 0.07 (SiMe_2), 10.70, 13.06, 14.58, 15.42 (C_5Me_4), 32.20 (CMe_3), 32.34 (CMe$_3$), 97.65, 101.13, 105.70, 107.38, 112.50, 113.74, 117.28, 122.94, 126.09, 149.29 (Cp). ^{2}H NMR (benzene): δ 4.48 (Zr-*D*). IR (benzene-d_6): ν = 1543 (Zr−H), 1108 cm^{-1} (Zr−D). ^{15}N NMR (benzene-d_6): δ = 655.04.

Acknowledgment. We thank the Department of Energy, Office of Basic Energy Sciences (DE-FG02-05-ER659) for financial support. P.J.C. is a Cottrell Scholar sponsored by the Research Corporation, a David and Lucille Packard Fellow in Science and Engineering, and a Camille Dreyfus Teacher−Scholar. T.E.H. was also partially supported by an NSF CSIP fellowship. We also acknowledge Cambridge Isotope Laboratories for a generous gift of $^{15}N_2$.

Supporting Information Available: Additional experimental and computational details. Crystallographic data for **1-N_2** and **1-H_2N_2** as CIF files. This material is available free of charge via the Internet at http://pubs.acs.org.

IC0620539